Pump-Probe Study on Nonlinear Switching in an All-Active-Semiconductor-Optical-Amplifier Loop Device

Jiun-Haw Lee, Ding-An Wang, Hsin-Jiun Chiang, Ding-Wei Huang, Steffen Gurtler, Yean-Woei Kiang, and C. C. Yang
Department of Electrical Engineering and Institute of Electro-Optical Engineering,
National Taiwan University, 1, Roosevelt Road, Sec. 4, Taipei, Taiwan, R.O.C.
Tel: 886-2-23657624 Fax: 886-2-23652637 E-mail: ccy@cc.ee.ntu.edu.tw

We report the pump-probe study results of the nonlinear switching behaviors in an all-active-semiconductor-optical-amplifier loop device as depicted in Fig. 1. The ridge-loading waveguide loop has a radius 300 μm with a ridge width 4 μm. The loop is connected to a multi-mode interference (MMI) waveguide with a length 500 μm and a ridge width 8 μm which serves as the nonlinear element. Then, the input and output ports are also 4 μm waveguides with both lengths about 100 μm. For injecting different currents in different areas, we divided the electro-pad into four disconnected regions, indicated by the injection currents I_1 (input/output region), I_2 (MMI region), I_3 (one-quarter of loop) and I_4 (three-quarter of loop). Figure 2 demonstrates three sets of data showing power-dependent switching. We launched a cw Ti:sapphire laser at 849.6 nm, which corresponded to the gain peak of the TE polarization, with various power levels and monitored the output power variation at the same wavelength. The horizontal axis in Fig. 2 shows the input power before entering the input waveguide. In this measurement, $I_1 = 30$ mA, $I_3 + I_4 = 300$ mA and the I_2 value is shown in the figure. Because the guiding layer of the amplifier waveguide was so thin (only about 0.3 μm), the input coupling efficiency was estimated to be only on the order of 0.1 % or even smaller. All three curves show depression of output power when the input power reaches certain values. The observed nonlinear switching behavior comes from the effect of the nonlinear coupling in the MMI waveguide region. This mechanism is different from that in a typical Sagnac interferometer which the nonlinear optical mechanism comes from the loop. The loop has the function of providing gain to the optical signals and redistributing the lateral wave field. Although the nonlinear optical mechanism comes from the MMI amplifier, the loop still plays a crucially important function. Figure 3 illustrates the simulation results for the four cases: loop with gain (normal function of the device), loop without gain (a small $I_3 + I_4$ for the device), mirror with gain (loop removed with an assumed gain), and mirror without gain (loop removed). We can see that only in the case of "loop with gain", efficient nonlinear switching can be observed.

Figures 4 shows the experimental setup for the cw pump-probe measurement. The two independent tunable Ti:Sapphire lasers were used to study the cross effect of two input signals of different wavelengths/polarization. The output signals passed a monochromator which was used as a spectral filter to eliminate the unwanted amplified spontaneous emission. In Fig. 5 (6), we demonstrate several sets of data with input power of the signal at 847.2 nm (849.6 nm) varied from 0 to 15 mW. The horizontal axis represents the input power at 849.6 nm (847.2 nm) and the vertical axis stands for the output power at the same wavelength. As shown in Fig. 5, the output power at 849.6 nm is affected by the input signal at 847.2 nm although the gain at 849.6 nm is higher. When the input power at 847.2 nm reaches 10 mW, the nonlinear switching effect becomes insignificant. On the other hand, from Fig. 6 the output power at 847.2 nm is not strongly affected by the input power at 849.6 nm.

In summary, we have fabricated all-semiconductor-optical-amplifier loop devices and characterized their operation with cw signals. Gain saturation in the MMI coupler led to nonlinear coupling and hence the power-dependent switching of the devices. The active loop is important to provide gain and to redistribute the field.

0-7803-5661-6 / 99 / $10.00 © 1999 IEEE

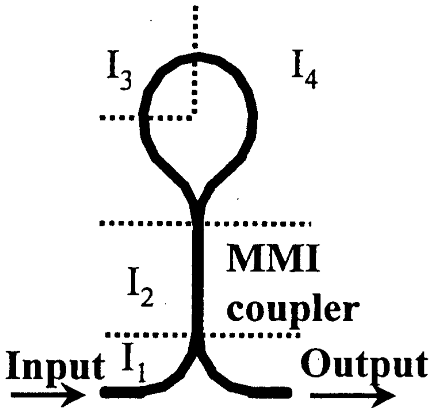

Fig.1 Layout of the device.

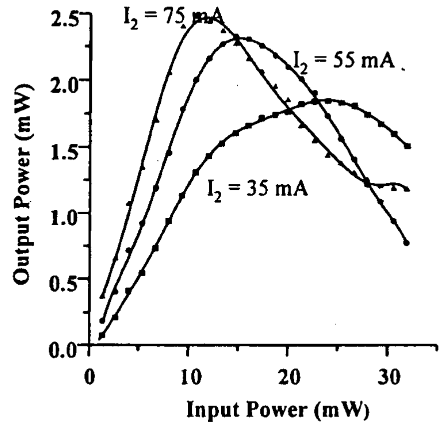

Fig.2 Output power as a function of input power with different I_2 values.

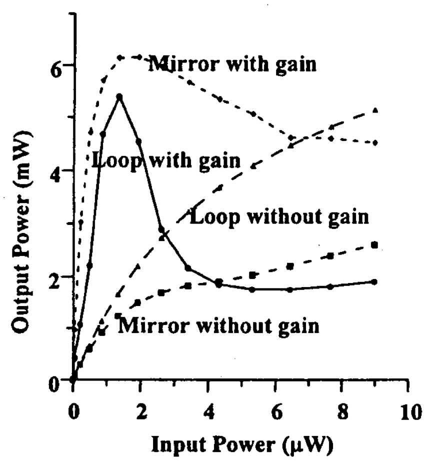

Fig.3 Simulation results with different device stuctures.

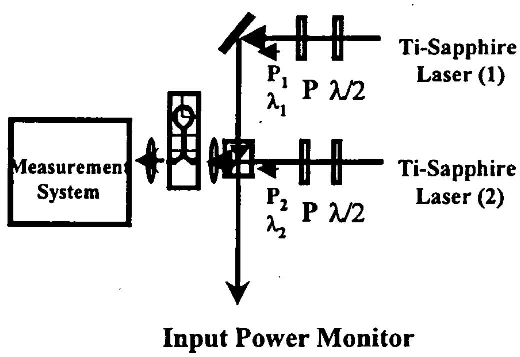

Fig.4 Experiment setup of cw pump-probe system.

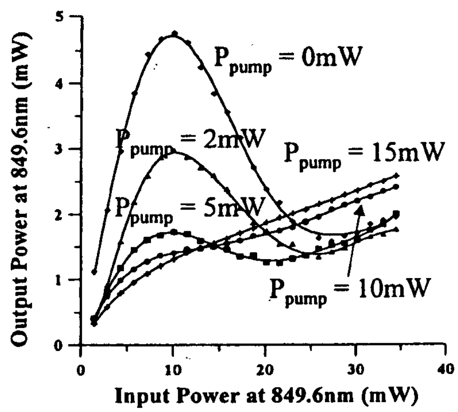

Fig.5 Output power as a function of input probe power (at 849.6 nm) with different input pump power (at 847.2 nm)

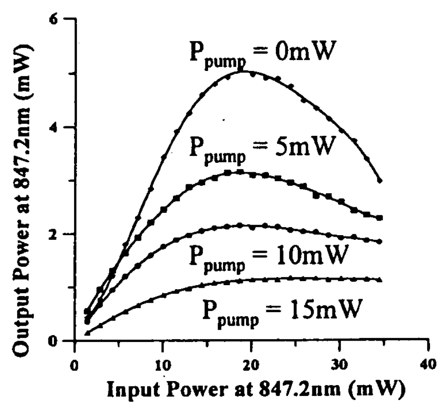

Fig.6 Output power as a function of input probe power (at 847.2 nm) with different input pump power (at 849.6 nm)